CXCL17 Chemokine-Dependent Mobilization of Memory CXCR8+CD8+ T_{EM} and T_{RM} Cells in the Vaginal Mucosa is Associated with Protection Against Genital Herpes

Ruchi Srivastava[1], **Marcela Hernández-Ruiz**[2], **Arif A. Khan**[1], **Mona A. Fouladi**[1], **Grace J. Kim**[1], **Vincent T. Ly**[1], **Yamada Taikun**[1], **Cynthia Lam**[1], **Bajarias S. Sarain**[1], **Undariya Boldbaatar**[1], **Albert Zlotnik**[2], **Elmostafa Bahraoui**[3,4], and **Lbachir BenMohamed**[1,5,6,*]

[1]Laboratory of Cellular and Molecular Immunology, Gavin Herbert Eye Institute, University of California Irvine, School of Medicine, Irvine, CA 92697

[2]Department of Physiology and Biophysics, University of California, Irvine, 3034 Hewitt Hall, Irvine, CA 92697

[3]NSERM, U1043, Toulouse, France CNRS, U5282, Toulouse, France

[4]Université Paul Sabatier Toulouse, Toulouse, France

[5]Department of Molecular Biology & Biochemistry, University of California Irvine, School of Medicine, Irvine, CA 92697

[6]Institute for Immunology, University of California Irvine, School of Medicine, Irvine, CA 92697

Abstract

Circulating conventional memory CD8+ T cells (i.e. the effector memory (CD8+ T_{EM}) and the central memory (CD8+ T_{CM}) subsets) and non-circulating tissue-resident memory CD8+ T cell subset (CD8+ T_{RM}) play a critical role in mucosal immunity. Mucosal chemokines, including the recently discovered CXCL17, are also important in mucosal immunity because they are homeostatically expressed in mucosal tissues. However, whether the CXCL17 chemokine contributes to the mobilization of memory CD8+ T cell subsets, to access infected mucosal tissues remains to be elucidated. Herein, we report that after intravaginal herpes simplex type 1 (HSV-1) infection of B6 mice, we detected high expression levels of CXCL17 and increased numbers of $CD44^{high}CD62^{Low}CD8^+$ T_{EM} and $CD103^{high}CD8^+$ T_{RM} cells, expressing CXCR8, the cognate receptor of CXCL17, in the vaginal mucosa (VM) of mice with reduced genital herpes infection and disease. In contrast to wild type B6 mice, the $CXCL17^{-/-}$ deficient mice developed: (*i*) fewer CXCR8+CD8+ T_{EM} and T_{RM} cells associated with more virus replication in the VM and more latency established in dorsal root ganglia (DRG); (*ii*) reduced numbers and frequencies of functional CD8+ T cells in the VM. These findings suggest that the CXCL17/CXCR8 chemokine pathway play a crucial role in mucosal vaginal immunity by promoting the mobilization of functional protective CD8+ T_{EM} and CD8+ T_{RM} cells, within this site of acute and recurrent herpes infection.

*Corresponding author: Dr. Lbachir BenMohamed, Laboratory of Cellular and Molecular Immunology, Gavin Herbert Institute; Hewitt Hall, Room 232; 843 Health Sciences Rd; Irvine, CA 92697-4390; Phone: 949-824-8937; Fax: 949-824-9626; Lbenmoha@uci.edu.

Conflict of interest: The authors have declared that no conflict of interest exists.

Keywords

Genital herpes; vaginal mucosa; CD8$^+$ T cells; CXCL17 and CXCR8

INTRODUCTION

Infections with herpes simplex virus type 1 and type 2 (HSV-1 and HSV-2) cause genital herpes disease, which affects more women than men (1–6). The prevalence of HSV-1 is much higher than HSV-2 with a staggering 3.72 billion individuals worldwide currently infected with HSV-1 (i.e., > 52% of the world population), (7, 8). HSV-1 is now becoming an increasing cause of genital herpes that accounts for close to 50% of new cases in developed countries (9, 10). After vaginal mucosa (VM) exposure, HSV-1 replicates in the mucosal epithelial cells thereby causing genital herpetic lesions. After clearance by the immune system the virus goes into a "steady-state" latent infection in the sensory neurons of dorsal root ganglia (DRG) where, in symptomatic individuals, it reactivates sporadically causing recurrent genital herpetic disease (7, 11). Recent work from our laboratory and others has demonstrated that inducing HSV-specific memory CD8$^+$ T cells in the VM tissue provides protection against genital herpes (10–13). However, the relative contribution of circulating conventional memory CD8$^+$ T cells (i.e. the effector memory (CD8$^+$ T$_{EM}$) and the central memory (CD8$^+$ T$_{CM}$ subsets) and non-circulating tissue-resident memory CD8$^+$ T cell subset (CD8$^+$ T$_{RM}$) in controlling mucosal herpes infection remains to be elucidated.

The mechanisms that regulate the mobilization of memory CD8$^+$ T$_{EM}$, CD8$^+$ T$_{CM}$, and CD8$^+$ T$_{RM}$ cells into infected vaginal mucosal tissues remain to be fully investigated (14, 15). Major gaps include the identity of chemokines that are involved and the underlying mechanisms through which these chemokines and their receptors mobilize protective memory CD8$^+$ T cell subsets into infected and inflamed mucosal tissues. Out of all 48 known human chemokines, CCL25, CCL28, CXCL14, and CXCL17 are especially important in mucosal immunity because they are homeostatically expressed in mucosal tissues (16, 17). Of these four mucosal chemokines, CXCL17 is the last member to have been identified and hence relatively little is known about its physiology (18–20). Its expression pattern suggests that it is a dual mucosal chemokine, with homeostatic and inflammatory functions (19, 21). CXCL17 is a polypeptide of 119 amino acid CXC chemokine whose cognate receptor was recently identified as GPR35/CXCR8 (19, 22). However, no information is currently available regarding the role of the CXCL17/CXCR8 signaling axis in mobilization of memory CD8$^+$ T$_{EM}$, CD8$^+$ T$_{CM}$, and CD8$^+$ T$_{RM}$ cells into infected or inflamed mucosal tissues. The vaginal mucosal tissues appear to be immunologically restricted and remain "a closed immunological compartment" resistant to accepting homing CD8$^+$ T cells that could be traveling from the draining lymph nodes and circulation (23, 24). Given the prominent and homeostatic expression of CXCL17 in the mucosal tissues, we hypothesized that: (*i*) CXCL17 may mobilize antiviral memory CXCR8$^+$CD8$^+$ T cells into HSV-1 infected vaginal mucosa; and (*ii*) such CXCR8$^+$CD8$^+$ T cells would contribute to protective immunity against genital herpes.

Our results revealed that HSV-1 infected and protected B6 mice developed increased frequency of HSV-specific IFN-γ-producing cytotoxic CXCR8$^+$CD8$^+$ T cells in the VM. Among these cells, increased number of CXCR8$^+$CD8$^+$ T$_{EM}$ and T$_{RM}$ cell subsets was associated with less virus replication in the VM and less latency established in DRG. In contrast, CXCL17$^{-/-}$ deficient mice developed fewer CXCR8$^+$CD8$^+$ T$_{EM}$ and T$_{RM}$ cells associated with increased virus replication in the VM and more latency established in DRG. Moreover, compared to wild type mice, reduced numbers and frequencies of functional CD8$^+$ T cells were detected in the VM of CXCL17$^{-/-}$ mice compared to wild type mice. These observations strongly propose the CXCL17/CXCR8 axis as promoting anti-viral T cell immunity at the vaginal mucosal tissue.

MATERIALS AND METHODS

Mice

CXCL17 deficient mice on the C57BL/6 background (CXCL17$^{-/-}$ mice, 5–6 weeks old, were kindly provided by Dr. Albert Zlotnik (University of California, Irvine). Female C57BL/6 (B6) mice (5–6 weeks old), were purchased from The Jackson Laboratory (Bar Harbor, ME). Animal studies conformed to the Guide for the Care and Use of Laboratory Animals published by the US National Institute of Health (IACUC protocol #2002-2372).

Virus production

Herpes simplex virus type 1 (HSV-1, strain McKrae) was grown and titrated on rabbit skin (RS) cells as previously described (10, 13, 14, 25).

Depo-Provera treatment

Mice were maintained on a 12-h dark and 12-h light cycle. Both groups of mice (CXCL17$^{-/-}$ and B6) were injected subcutaneously (1X) with two mg progesterone (Depo-Provera$^®$), to synchronize the ovarian cycle and increase susceptibility to herpes infection, and then received an IVAG HSV-1 challenge (26).

Intravaginal infection

After Depo-Provera$^®$ subcutaneous (SC) treatment, groups of age-matched female CXCL17$^{-/-}$ and C57BL/6 mice were infected intravaginally (IVAG) with 2×10^5 plaque forming units (PFU) of HSV-1 (strain McKrae). Twenty µl of virus suspension were instilled intravaginally using a pipette with a sterile plastic tip.

Vaginal wash collection

Vaginal washes were collected on days 3, 5, 8, 12, and 18 post-infection by pipetting 30 µL. of phosphate-buffered saline (PBS) in and out of the vagina three times and were frozen at −80°C.

Viral titer assay

Vaginal washes were analyzed for viral titers by plaque assays. Vero cells were grown in α-modified Eagle's medium (ThermoFisher Scientific, Waltham, MA) supplemented with 5%

fetal bovine serum and 1% penicillin-streptomycin, and L-glutamine (ThermoFisher Scientific). For plaque assays, Vero cells were grown to confluence in 24-well plates. Vaginal wash samples were diluted and added to monolayers. Infected monolayers were incubated for 1 h at 37°C and were rocked every 15 min for viral absorption. Infected monolayers were overlaid with an overlay media containing carboxy-methyl cellulose. Infection was allowed to occur for 72 h at 37°C. Monolayers were then fixed and stained with crystal violet, and viral plaques were counted under a light microscope. Positive controls were run with every assay with previously titered laboratory stocks of HSV-1.

Clinical Score

Mice were examined for vaginal disease after the HSV-1 challenge. Vaginal disease was determined by a masked investigator on days 1, 3, 5, 8, 12, and 18 thereafter. A standard 0–4 scale was used: 0, no disease; 1, 25%; 2, 50%; 3, 75%; and 4, 100%, disease respectively.

Isolation of lymphocytes

Lymphocytes were isolated from the female vaginal mucosa (VM) tissues and treated with calcium- and magnesium-free phosphate-buffered saline (PBS) for whole-body perfusion prior to tissue harvest, as previously described (27). The vaginal mucosa was excised from the group of mice and tissue was cut longitudinally and minced with a sterile scalpel in complete tissue culture. Minced tissues were digested in complete medium containing 2.5 mg/ml collagenase type IV (Sigma Chemical Co., St. Louis, MO.). Digestion was accomplished by shaking incubation at 37°C for 30 min after which tissues and cells were filtered through a sterile gauze mesh and washed with RPMI 1640 medium. Spleen and draining lymph node homogenates were prepared by pressing the tissue through a sterile mesh screen into ten mL of PBS under aseptic conditions.

Quantitative RT-PCR

Total RNA was extracted from each mouse vagina sample using TRIzol® (Invitrogen, Carlsbad, CA). Equal concentrations of RNA were used for the reverse transcription reaction to generate cDNA (Qiagen, Valencia, CA). Quantitative real-time PCR (q-PCR) data was generated with a Roche LightCycler® 480 using a Universal Probe Library-based system. Seventy ng of each cDNA was used per 40 cycle PCR run. Gene-specific primers and corresponding Universal Probes were used in every reaction to quantify the amount of *CXCL17, CXCL14, CCL28, CXCL1, CXCL2, CXCL9, CXCL10, CCL2, CCL3, CCL5 and actin* gene transcripts in each tissue sample. Data was analyzed by performing relative quantification and graphed using GraphPad Prism software (www.graphpad.com).

Flow cytometry

Single cell suspensions from the spleen, lymph node and vaginal mucosa, were prepared for flow cytometric analysis. The following antibodies were used: anti-mouse CD8 PerCP (clone 53-6.7, BD Biosciences, San Jose, CA), anti-mouse CD11a FITC (clone M17/4, BD Biosciences), anti-mouse CD103 APC (clone M290, BD Biosciences) anti-mouse CD62L A700 (clone MEL-14, BD Biosciences) anti-mouse CD44 APC-cy7 (clone IM7, BioLegend, San Diego, CA), anti-mouse CD69 PE-cy7 (clone H1.2F3, BD Biosciences), anti-mouse

CCR7 A647 (clone 4B12, BD Biosciences), TIGIT PE (clone GIGD7, eBioscience), VISTA (clone 13f3, a gift from Dr. Noelle, Geisel School of Medicine at Dartmouth, Lebanon, NH), TIGIT, CD107[a] FITC (clone ID4B, BD Biosciences), CD107[b] FITC (clone M3/84, BD Biosciences) and anti-mouse IFN-γPE-cy7(clone XMG1.2, BioLegend). For surface staining, mAbs were added against various cell markers to a total of 1×10^6 cells in phosphate-buffered saline containing 1% FBS and 0.1% Sodium azide (fluorescence-activated cell sorter [FACS] buffer) and left for 45 min at 4°C. For intracellular staining cells were first treated with cytofix/cytoperm (BD Biosciences) for 30 min. Upon washing with Perm/Wash buffer, mAbs were added to the cells and incubated for 45 min on ice and in the dark. Cells were washed again with Perm/Wash and FACS buffer and fixed in PBS containing 2% paraformaldehyde (Sigma-Aldrich, St. Louis, MO).

For the measurement of CD107[a/b] and IFN-γ, 1×10^6 cells were first transferred into 96-well flat bottom plate in the presence of BD GolgiStop (10 μg/ml) for 6 h at 37°C. Phytohemagglutinin (PHA) (5 μg/ml) (Sigma-Aldrich) was used as positive control. At the end of the incubation period, the cells were transferred to a 96-well round bottom plate and washed once with FACS buffer. Surface and intracellular staining were performed as aforementioned. A total of 100,000 events were acquired by the LSRII (Becton Dickinson, Mountain View, CA) followed by analysis using the FlowJo software (TreeStar, Ashland, OR).

Statistical analysis

We examined the distribution of each immunological parameter as we previously described (10). In the case of two group comparisons, we have considered the use of the parametric two-sample Student's *t*-test or non-parametric Wilcoxon rank sum test. In addition, for paired comparisons involving multiple peptides, we have adjusted for multiple comparisons using the Bonferroni procedure. In the specific case of three groups (comparing two subgroups with a baseline subgroup) we have used the General Linear Model procedure and compared the least squares means using the Dunnett procedure for multiple comparisons. Flow cytometry data were analyzed with FlowJo software (TreeStar). For analysis, we used SAS® v.9.4 (Statistical Analysis System, Cary, NC). Graphs were prepared with GraphPad Prism software (San Diego, CA). Data are expressed as the mean ± SD. Results were considered to be statistically significant at $p < 0.05$.

RESULTS

1. Frequent CD8^{+} T cells, expressing CXCR8, the cognate receptor of CXCL17, are detected in the vaginal mucosa of HSV-1 infected protected mice

Both HSV-1 and HSV-2 cause genital herpes lesion. We chose HSV-1 for this study because it is present in more than 3.7 billion people worldwide and, besides HSV-2, HSV-1 is becoming in recent years an increasing cause of genital herpes that accounts for half of new cases in developed countries (9, 10).

We first performed a dose-response study of infection with HSV-1 (strain McKrae) in a group of female B6 mice ($n = 10$) were using 1×10^5, 2×10^5 or 5×10^5 plaque forming

units (PFU), delivered intravaginally (IVAG) in PBS. An illustration of the infection scheme and the timeline of subsequent immunological and virological assays are shown in Fig. 1A. All three doses induced a similar magnitude of T cell responses in the vaginal mucosa (VM) and in the spleen (SPL). Moreover, with the 2×10^5 PFU dose; about half of the animals developed severe genital herpes disease (score above 1 on a scale of 0 to 4) (non-protected) while the other half of the animals had no genital herpes disease (scored 0) (protected) (Figs. 1B and 1C). Most genital herpes lesions are associated to virus replication in the vaginal mucosa. The lack of genital herpes lesions in protected mice was not due to a lack of infection because the virus was readily detected in the vaginal swabs of most animals (Fig. 1D). Accordingly, intravaginal HSV-1 infections in all subsequent experiments were carried out using the middle dose of 2×10^5 PFU.

In a subsequent experiment, a group of female B6 mice ($n = 30$) were infected intravaginally with 2×10^5 PFU HSV-1 and then segregated into protected and non-protected groups as in Figs. 1A and 1B, above. Cell suspensions ($\sim 10 \times 10^6$) derived from the vaginal mucosa (VM) of HSV-1 infected mice were harvested and the levels of mRNA of nine T-cell attracting and mucosal chemokines (CXCL1, CXCL2, CXCL9, CXCL10, CXCL14, CXCL17, CCL2, CCL3, CCL5 and CCL28) were analyzed by PCR, as described in the *Materials and Methods section*. As shown in Fig. 2A, compared to other eight mucosal chemokines, the mRNA from CXCL17 was by far the highest chemokine expressed in the vaginal mucosa of HSV-1 infected B6 mice. A low basal level of CXCL17, but relatively higher compared to other chemokines, was also detected in the uninfected vaginal mucosa of B6 mice (*not shown*).

Next, a group of female B6 mice ($n = 30$) were infected intravaginally with 2×10^5 PFU HSV-1 and then segregated into protected and non-protected groups as in Figs. 1A and 1B, above. We then compared by FACS the level of expression of CXCR8, the cognate receptor of CXCL17 on $CD8^+$ T cells, and the frequencies of $CXCR8^+CD8^+$ T cells in cell suspensions from the VM and SPL (used as control) of protected ($n = 10$) versus non-protected mice ($n = 10$). Significantly high levels of CXCR8 were detected on $CD8^+$ T cells from the VM of protected mice compared to non-protected mice (Figs. 2B and 2C). Moreover, frequent $CXCR8^+CD8^+$ T cells were also detected in the VM of protected mice compared to non-protected mice (Figs. 2D and 2E). In contrast to VM tissue, levels of CXCR8 and similar frequencies of $CXCR8^+CD8^+$ T cells detected in the SPL of protected and non-protected mice were not significant. Taken together, these results suggest that the recently discovered CXCL17 mucosal chemokine is associated with the mobilization of protective memory $CXCR8^+CD8^+$ T cells within inflamed and infected vaginal mucosal tissue.

2. Frequent memory $CD8^+$ T_{EM} and $CD8^+$ T_{RM} cells detected in the vaginal mucosa of HSV-1 infected protected, compared to non-protected mice

We next determined the relative contribution of the conventional memory $CD8^+$ T cells (i.e. $CD8^+$ T_{CM} and $CD8^+$ T_{EM}) and the non-circulating tissue-resident memory $CD8^+$ T_{RM} in the protection against genital herpes. A group of female B6 mice ($n = 30$) were infected intravaginally with 2×10^5 PFU HSV-1 and then segregated into protected and non-

protected mice, as in Figs. 1A and 1B, above. Protected and non-protected animals were sacrificed on day 21 and the frequencies of HSV-1 $gB_{498-505}$ epitope-specific $CD8^+$ T_{CM}, $CD8^+$ T_{EM} and $CD8^+$ T_{RM} cells were compared by FACS in cell suspensions from the VM (the site of acute HSV infection), the dorsal root ganglia (DRG, the site of HSV latency) and SPL of protected ($n = 10$) and non-protected mice ($n = 10$).

More $CD44^{high}CD62^{high}CD8^+$ T_{CM} were detected in the VM of non-protected compared to VM of protected mice (Figs. 3A, 3B and 3G, $P = 0.04$). In contrast, significantly higher numbers of $gB_{498-505}$-specific $CD44^{high}CD62^{Low}CD8^+$ T_{EM} (Figs. 3C, 3D and 3G) and $CD103^{high}CCR7^{low}CD62L^{low}CD11a^{high}CD69^{high}CD8^+$ T_{RM} cells (Figs. 3E, 3F and 3G) were detected in both the VM and DRG of protected as compared to non-protected mice ($P = 0.04$). There were no differences in the number and percentage of $gB_{498-505}$-specific T_{EM} and T_{RM} cells in the SPL of protected vs. non-protected mice (Fig. 3G, *right panels*). As a control, no significant $CD8^+$ T cells specific to the irrelevant target $OVA_{257-264}$ peptide were detected in protected and non-protected mice, demonstrating the HSV specificity of the $CD8^+$ T cells (*data not shown*). Altogether, these results indicate that mobilization of HSV-specific $CD44^{high}CD62^{Low}CD8^+$ T_{EM} and $CD103^{high}CCR7^{low}CD62L^{low}CD11a^{high}CD69^{high}CD8^+$ T_{RM} cells into vaginal mucosal and dorsal root ganglia is associated with protection against genital herpes lesions.

3. Frequent HSV-specific IFN-γ-producing cytotoxic CD8+ T cells in the vaginal mucosa is associated with protection against genital herpes

A group of female B6 mice ($n = 30$) were infected intravaginally with 2×10^5 PFU HSV-1 and then segregated into protected and non-protected groups as in Figs. 1A and 1B, above. The VM and SPL (control) were harvested from 10 protected and 10 non-protected mice on day 21 post-infection. The frequency of IFN-$\gamma^{(+)}$ $CD8^+$ T cells and $CD107^{(+)}$ $CD8^+$ T cells were compared in protected and non-protected mice by FACS using the gating strategy shown in Fig. S2, as previously described (10). A significant increase in the percentage ($P < 0.05$) and numbers ($P = 0.03$) of HSV-1 $gB_{498-505}$-specific $CD107^{(+)}CD8^+$ T cells (Figs. 4A and 4B, left panel) and IFN-$\gamma^{(+)}$ $CD8^+$ cytotoxic T cells ($P = 0.03$, Figs. 4C and 4D, *middle panel*) were detected in the VM of protected mice vs. non-protected mice. As expected, cells from both VM and SPL that were not stimulated with peptide showed non-significant numbers of $CD107^{(+)}$ and IFN-$\gamma^{(+)}$ $CD8^+$ T cells (Figs. 4A–4D, *right panel*). These results suggest that a significant increase in functional IFN-γ-producing cytotoxic $CD8^+$ T cells in the VM is associated with protection against genital herpes.

4. CXCL17$^{-/-}$ deficient mice develop significantly less memory CXCR8+CD8+ T cells and more acute and latent herpes infection compared to wild type mice

We next determined whether the lack of CXCL17 would affect $CD8^+$ T_{CM}, $CD8^+$ T_{EM} and $CD8^+$ T_{RM} cells mobilization, the viral titers in the vaginal mucosa and the load of latent viral infection in the DRG of HSV-1 infected CXCL17$^{-/-}$ deficient mice. A group of age-matched CXCL17$^{-/-}$ deficient and wild type (WT) B6 mice ($n = 10$) were infected intravaginally with 2×10^5 PFU of HSV-1 (Fig. 5A). Virus replication in the VM (the site of HSV acute replication) and the level of latency that developed in the dorsal root ganglia (DRG, the site of HSV latency) were compared in CXCL17$^{-/-}$ deficient and wild type (WT)

B6 mice. The frequency of HSV-specific CXCR8$^+$CD8$^+$ T cells and the level of expression of CXCR8 on CD8$^+$ T cells, the receptor of CXCL17 mucosal chemokine, were also compared in the VM compartment of CXCL17$^{-/-}$ and WT mice.

Viral titers measured in vaginal swabs taken on days 3, 5, 8, 12 and 18 post-infection (Fig. 5A) demonstrated a significant less control of virus replication leading to more genital herpes infection in CXCL17$^{-/-}$ mice compared to WT mice ($P < 0.05$, Fig. 5B). CXCL17$^{-/-}$ mice developed severe genital lesions (average score of 3 on a scale of 0 to 4) compared to WT mice (average score of 2). Moreover, the level of latency established in DRG of CXCL17$^{-/-}$ mice was also significantly high than that was established in DRG of WT mice ($P < 0.05$, Fig. 5C). Moreover, significantly less CXCR8$^+$CD8$^+$ T cells were detected in the VM of CXCL17$^{-/-}$ mice compared to WT mice ($P = 0.04$). (Figs. 5D and 5E). Compared to CD8$^+$ T cells from WT mice, CD8$^+$ T cells in the VM of CXCL17$^{-/-}$ mice expressed significantly low levels of CXCR8 receptor ($P = 0.04$, Figs. 5F and 5G). In contrast to VM compartment, similar low frequencies of CXCR8$^+$CD8$^+$ T cells and low level of CXCR8 expression were detected in the SPL of CXCL17$^{-/-}$ compared to WT mice. These results indicated that: (*i*) a CXCL17-dependent mobilization of HSV-specific CXCR8$^+$CD8$^+$ T cells in the vaginal mucosa following intravaginal infection with HSV-1; (*ii*) lack of CXCL17 chemokine is associated with an increased genital herpes infection and more latency established in the DRG.

5. Mobilization of memory CD8$^+$ T$_{CM}$, CD8$^+$ T$_{EM}$, and CD8$^+$ T$_{RM}$ cell subsets in the vaginal mucosa of HSV-1 infected CXCL17$^{-/-}$ deficient mice is compromised

We next determined whether the lack of CXCL17 chemokine would affect the mobilization of conventional CD8$^+$ T cells (i.e. CD8$^+$ T$_{CM}$ cells and CD8$^+$ T$_{EM}$ cells) and tissue-resident memory CD8$^+$ T$_{RM}$ cells in the VM (the site of HSV acute replication) and the dorsal root ganglia (DRG, the site of HSV latency). The spleen (SPL) was used as control.

A group of age-matched CXCL17$^{-/-}$ deficient and WT mice ($n = 10$) were infected intravaginally with 2×10^5 PFU of HSV-1, as in Fig. 5A above. All animals were sacrificed on day 21 post infection and the frequencies of HSV-1 gB$_{498-505}$ epitope-specific CD8$^+$ T$_{CM}$, CD8$^+$ T$_{EM}$ and CD8$^+$ T$_{RM}$ cells were compared by FACS in the VM, DRG and SPL (control) of ten CXCL17$^{-/-}$ and ten WT mice, using the gating strategy shown in Fig. S3.

Significantly lower numbers of gB$_{498-505}$-specific CD44^{high}CD62^{high}CD8$^+$ T$_{CM}$ cells (Figs. 6A, 6B and 6G) and CD44^{high}CD62^{Low}CD8$^+$ T$_{EM}$ cells (Figs. 6C, 6D and 6H) were detected in both the VM and DRG of CXCL17$^{-/-}$ deficient mice compared to WT mice ($P = 0.04$). Although the numbers of gB$_{498-505}$-specific T$_{RM}$ cells detected in VM and DRG of WT vs. CXCL17$^{-/-}$ deficient mice was low compared to T$_{CM}$ and T$_{EM}$ cells, there was significantly lower percentages of T$_{RM}$ cells in CXCL17$^{-/-}$ mice compared to WT mice ($P = 0.04$). (Figs. 6E, 6F and 6I). Similar frequencies of memory CD8$^+$ T cell subsets were detected in the SPL (control) of CXCL17$^{-/-}$ mice compared to WT mice (Figs. 6G, 6H and 6I, left panels). Altogether, these results indicate that mobilization of HSV-specific specific T$_{CM}$, T$_{EM}$ and T$_{RM}$ cells into the vaginal mucosal and dorsal root ganglia is CXCL17-dependent.

6. Reduced numbers and frequencies of functional CD8⁺ T cells detected in the vaginal mucosa of CXCL17⁻/⁻ deficient mice compared to wild type mice

A group of age-matched CXCL17$^{-/-}$ deficient and wild type (WT) B6 mice ($n = 10$) were infected intravaginally with 2×10^5 PFU HSV-1 as in Fig. 5A) above. All animals were sacrificed on day 21 and the frequency of IFN-γ$^+$CD8$^+$ T cells and of CD107$^+$ CD8$^+$ T cells were compared in the VM and SPL (control) of CXCL17$^{-/-}$ and WT B6 mice by FACS assay, as above. CD8$^+$ T cells were also analyzed by FACS for expression of markers of exhaustion, including T cell Ig and ITIM domain (TIGIT) and V-domain Ig suppressor of T cell activation (VISTA) (28–30).

A significant decrease in the percentage and numbers of both HSV-1 gB$_{498-505}$-specific CD107$^+$ CD8$^+$ T cytotoxic T cells and IFN-γ$^+$CD8$^+$ T cells were detected in the VM of CXCL17$^{-/-}$ mice compared to WT mice (P 0.04, Figs. 7A–7D, *top panels*). In contrast, significant differences were not detected in the SPL of CXCL17$^{-/-}$ mice compared to WT mice ($P > 0.05$, Figs. 7A–7D, *lower panels*). There was a ~two-fold increase in VM-resident TIGIT$^+$CD8$^+$ T cells from CXCL17$^{-/-}$ mice as compared to WT mice ($P < 0.05$, Figs. 7E and 7F, *top panels*). There was also an approximately two-fold increase in VM-resident VISTA$^+$CD8$^+$ T cells from CXCL17$^{-/-}$ as compared to WT B6 mice ($P = 0.05$, Figs. 7G and 7H, *top panels*). In contrast, no significant differences were detected in the SPL of CXCL17$^{-/-}$ mice compared to WT mice ($P > 0.05$, Figs. 7E to 7H, *lower panels*). Accordingly, the tetramer staining detected significantly lower percentage ($P = 0.04$) and number ($P = 0.03$) of HSV-1 gB$_{498-505}$ epitope-specific CD8$^+$ T cells in the vaginal mucosa of CXCL17$^{-/-}$ deficient mice compared to the vaginal mucosa of WT mice (Fig. S1).

These results demonstrated that a lack of CXCL17 chemokine is associated with: (*i*) a significant decrease in the effector functions (IFN-γ production and CD107$^{a/b}$ degranulation) of HSV-specific CD8$^+$ T cells in the VM of HSV-1 infected CXCL17$^{-/-}$ deficient mice; (*ii*) a significant increase in the HSV-specific CD8$^+$ T cells expressing markers of exhaustion in the VM of CXCL17$^{-/-}$ mice. Thus, lack of CXCL17 appeared to be associated with reduced numbers and frequencies of functional HSV-specific CD8$^+$ T cells in the vaginal mucosa of CXCL17$^{-/-}$ deficient mice.

DISCUSSION

In this study, we demonstrated that the CXCL17 mucosal chemokine is involved in the mobilization of HSV-specific CXCR8$^+$CD8$^+$ T$_{EM}$ and T$_{RM}$ cells within the vaginal mucosa and this was associated with protection against genital herpes. Strong local production of CXCL17 appeared to be associated with the mobilization CXCR8$^+$CD8$^+$ T$_{EM}$ and T$_{RM}$ cell subsets within the VM of B6 mice with impaired HSV-1 replication in the VM, less severe genital lesions and reduced latency established in DRG. In contrast, when compared to WT B6 mice, the CXCL17$^{-/-}$ deficient mice developed significantly less frequent CXCR8$^+$CD8$^+$ T$_{EM}$ and T$_{RM}$ cell subsets in the vaginal mucosa associated with more HSV-1 replication, severe genital lesions and more latency established in DRG. Furthermore, a significant deficiency in the functions (IFN-γ production and CD107$^{a/b}$ degranulation) of CD8$^+$ T cells was observed in the VM of CXCL17$^{-/-}$ deficient mice, which failed to contain genital herpes infection and disease. These results demonstrate for the first time that the CXCL17/

CXCR8 chemokine axis is of paramount importance in the mucosal immunity, mobilizing protective $CXCR8^+CD8^+$ T_{EM} and T_{RM} cells to the mucosal tissues associated with clearance of genital herpes infection and disease. The results also suggest an opportunity to develop a T-cell based genital herpes prime/pull vaccine based on immunization that would specifically induce functional HSV-specific $CD8^+$ T_{EM} and T_{RM} cell subsets combined with an intravaginal delivery of mucosal chemokines, such as CXCL17, that would mobilize these $CD8^+$ T_{EM} and T_{RM} cells into infected vaginal mucosa.

Following the resolution of viral mucosal infections, long-lived heterogeneous memory $CD8^+$ T cell population is generated (38–42). This heterogeneous memory $CD8^+$ T cell population can be divided into three major subsets: Circulating conventional (1) effector memory ($CD8^+$ T_{EM}) and (2) central memory ($CD8^+$ T_{CM}) subsets and (3) the non-circulating tissue-resident memory $CD8^+$ T cell subset ($CD8^+$ T_{RM}) (23). The three subsets of memory T cells differ in their phenotype, function, and anatomic distribution. The T_{CM} cells are $CD103^{low}CD62L^{high}CCR7^{high}$. The T_{EM} cells are $CD103^{low}CD62L^{low}CCR7^{low}$. The T_{RM} cells are $CD103^{high}CD62L^{low}CCR7^{low}CD11a^{high}CD69^{high}$ (23, 43–45). Once formed, T_{RM} cell subset do not re-enter the circulation and therefore play an essential role in locally guarding mucosal tissues from secondary infections. The precise mechanisms by which the three memory $CD8^+$ T cell subsets are formed, maintained, and expanded remains to be elucidated. In humans, $CD8^+$ T cells are rapidly recruited into the vaginal mucosal following infection. After clearance of primary infection, the memory $CD8^+$ T cells then develop and persist in the vaginal mucosal tissue, at the dermal-epidermal junction (35). In this study, we found that high frequencies of HSV-specific memory $CD8^+$ T_{EM} and $CD8^+$ T_{RM} cells get retained in the vaginal mucosa of HSV-1-infected and protected WT mice, impairing HSV-1 replication in the VM and causing less severe genital lesions with reduced latency established in DRG. This is in sharp contrast to HSV-1-infected and non-protected CXCL17 deficient mice, with more HSV-1 replication in the VM causing severe genital lesions and increased latency established in DRG. This suggests that these HSV-specific memory $CD8^+$ T_{EM} and $CD8^+$ T_{RM} cells may control local viral replication and disease at the site of vaginal mucosal herpes lesions which consequently led to lower level of latent viral load established in DRG.

The expression pattern of CXCL17 in human tissues and cells indicates that it is a mucosa-associated chemokine (19, 21). In this study, our data revealed that CXCL17 is the most highly expressed chemokine in the vaginal mucosa of HSV infected mice. This novel observation points to a unique role of CXCL17 chemokines in vaginal T cell immunity and prompted us to focus on its role in the mobilization of memory $CD8^+$ T_{EM}, $CD8^+$ T_{CM} and $CD8^+$ T_{RM} cells into the vaginal mucosal tissue (23). Only a handful of reports have described the immune-biology of CXCL17 because it is the last mucosal chemokine to be identified (18–20). CXCL17 is regulated by vascular endothelial growth factor and is chemotactic for both macrophages and dendritic cells (46). CXCL17 signals through the previously identified orphan G protein-coupled receptor-35 (GPR35), which has been renamed CXCR8 (19). Human and mouse CXCL17, which share 71% sequence identity at the amino acid level, are homeostatically expressed in certain mucosal sites (trachea, bronchus and stomach), but induced upon inflammation in others (intestine) (21). It is therefore a dual (homeostatic/inflammatory) chemokine (16, 17). We also found CXCR8 to

be highly expressed on vaginal mucosa-resident CD8$^+$ T cells of HSV-1 infected protected mice as compared to non-protected mice. Intravaginal HSV infection resulted in the recruitment of more CXCR8$^+$CD8$^+$ T cells to the inflamed vaginal mucosa of protected mice compared to non-protected mice. These intriguing results allow us to suggest that the CXCL17/CXCR8 axis plays a crucial role in the mobilization of functional HSV-specific CXCR8$^+$CD8$^+$ T$_{EM}$ cells and HSV-specific CXCR8$^+$CD8$^+$ T$_{RM}$ cells to the infected vaginal mucosa. Such mobilization was associated with significantly less HSV-1 replication in the vaginal mucosa and less latency established in DRG. While chemokine selection in the present study was narrowed to a small panel of chemokines, the expression of all other known 48 chemokines in the vaginal mucosa will be studied using NanoString and Luminex assays and their functional role in herpes T cell immunity will be subject to future reports.

CD8$^+$ T cells are maintained in the dermal-epidermal junction in women's vaginal mucosa and mediate protection against genital herpes (10, 13, 31–37). The small number of gB$_{498–505}$-specific CD8$^+$ T cells detected in the vaginal mucosa could be related to the route of infection used (i.e. intravaginal instead of skin infection) and to the slight compartmentalization of T cells in the vaginal mucosa, which seems to be a "closed immunological compartment". Compartmentalization of HSV-specific CD8$^+$ T cells in the vaginal mucosa might require stronger activation, mobilization and retention compared to other compartments such as skin and lymphoid organs (e.g. genital tract draining lymph nodes). Moreover, exhaustion of these CD8$^+$ T cells is likely a major factor that interferes with T cell-mediated immune surveillance at the VM and contributes to failure to control persistent infections, such as HSV-1. High expression of T-cell co-inhibitory receptors, including VISTA, TIGIT, PD-1 and TIM-3 might be associated with functional exhaustion of T cells. TIGIT and VISTA are newly discovered T-cell co-inhibitory receptors (28–30). TIGIT binds with high affinity to CD155 on dendritic cells (DC) and macrophages (MΦ). During HIV infection, TIGIT expressing CD8$^+$ T cells are associated with clinical markers of HIV disease progression (47). It has recently been demonstrated that VISTA is also an immune checkpoint molecule for human T cells (29). VISTA-Ig interaction suppresses activation of tumor-specific T cells (29). In the present study, we found high expression levels of both VISTA and TIGIT on vaginal mucosa-resident CD8$^+$ T cells that reside in the VM of CXCL17$^{-/-}$ deficient mice as compared to WT mice. These CD8$^+$ T cells retained a reduction in both IFN-γ production and cytotoxic activity associated with a lack of protection against genital herpes infection and disease. These results suggest a persistent antigenic stimulation in CXCL17$^{-/-}$ deficient mice. To the best of our knowledge, this is the first study to show that expression of VISTA and TIGIT on HSV-specific memory CD8$^+$ T cells is associated with a lack of protective immunity against genital herpes. It is likely that a CXCL17-dependent exhaustion of the existing CD8$^+$ T cells might reduce their proliferation which in turn might contribute to a low number of CXCR8$^+$CD8$^+$ T cells seen in the vaginal mucosa of CXCL17$^{-/-}$ mice. Nevertheless, the mechanism by which the lack of CXCL17 mucosal chemokine led to increased expression of VISTA and TIGIT on vaginal mucosa-resident CD8$^+$ T cells remains to be elucidated. Our results suggest that the co-blockade of VISTA and TIGIT pathways should further be explored to elicit potent anti-viral CD8$^+$ T cell effector functions to potentially control genital herpes.

In this study, mice were treated with Depo-Provera®, a progestational formulation. Progesterone is widely used to synchronize the ovarian cycle and to increase susceptibility to genital herpes infection in mice (1, 2). Vaginal infection in the progesterone-treated mouse model appears to mimic the infection in humans (3, 4). Since both protected mice and unprotected mice were similarly treated with Depo-Provera, it is unlikely that the proportion of "protected" and "unprotected" mice was directly related to the progesterone treatment. Nevertheless, one might not exclude some variations in susceptibility to genital herpes infection within the same group of progesterone-treated mice (e.g. Fig. 1C). Moreover, it is possible that the timing of Depo-Provera® treatment relative to infection might affect susceptibility to genital herpes infection and, hence, the level of protection. However, kinetic studies to determine whether timing affects the effect of progesterone treatment on susceptibility to genital herpes infection remains outside the scope of the present study, and hence should be addressed in future studies.

Some dichotomous results in protection within same group of mice are recorded. As shown in Fig. 1C, although the majority of mice in the protected group had low genital lesion (score 1) to no disease (score 0), it occurs that one mouse did show a medium score of 2. Although (i) the viral inoculum is constant as the same batch was used throughout the experiments, and (ii) the scoring of genital lesions was performed by the same person; one cannot not exclude some variations within the same group of mice. These variations could be related to lack of synchronized ovarian cycle within the same group of progesterone-treated mice, and/or to intrinsic experimental effects, for instance, due to mechanical lesions of the mucosa during the vaginal instillation of the viral inoculum. These variations can occur even when an inbred B6 mouse strain are used.

Once the acute infection is cleared in the vaginal mucosa, the site of acute infection, the virus stays dormant in DRG, the site of latent infection. In CXCL17$^{-/-}$ deficient mice, we detected high levels of viral replication in the vaginal mucosa and high level of latency in DRG. The differences in viral load in the vaginal mucosa and DRG of CXCL17$^{-/-}$ deficient mice vs. WT mice are associated to quantitative and qualitative differences in CXCL17-dependent mobilization of memory CXCR8$^+$CD8$^+$ T_{EM} and T_{RM} cells. Since only hundreds of neuronal cells are latently infected in DRG, fewer T cells might be needed in DRG compartment, compared to vaginal mucosa compartment, to reduce the level of latent viral load. Thus, although lower frequency of CD8$^+$ T_{EM} and T_{RM} cells was detected in the DRG compared to the vaginal mucosa of CXCL17$^{-/-}$ deficient mice, these fewer cells seem to be sufficient to reduce the level of latent viral load in DRG. However, in the vaginal mucosa, where there is an abundance of infected cells, more CD8$^+$ T_{EM} and T_{RM} cells might be required to significantly reduce the level of viral load. Moreover, it is likely that CXCL17 might not be the only chemokine that operates in attracting T_{EM} and T_{RM} cells to vaginal mucosa. Besides, CXCL17, other mucosal chemokines, including CCL14, CCL25 and CCL28, might also be involved in T-cell recruitment to the vaginal mucosa. Hence, CXCL17 might synergistically or additively operate with other mucosal chemokines to attract T_{EM} and T_{RM} cells to the vaginal mucosa. Although a decrease in T_{CM} cells is also detected in the vaginal mucosa of CXC17$^{-/-}$ mice, this decrease was not as pronounced as for the other two subsets of T cells (i.e. T_{EM} and T_{RM} cells).

Mucosal surfaces represent the entry route of many viral pathogens, such as HSV-1 and HSV-2. Although both HSV-1 and HSV-2 cause genital herpes lesion, we chose HSV-1 for this study because it is present in more than 3.7 billion people worldwide and is becoming an increasing cause of genital infection in developed countries (9, 10). HSV-1 is also the cause of cold sores around the mouth and most serious HSV-1 infection of the eye that can lead to potentially blinding ocular herpetic disease (11). Controlling the spread of genital herpes remains a challenge despite the availability of many intervention strategies, such as sexual behavior education, barrier methods, and the daily guanine nucleoside anti-viral drug therapies (e.g. Acyclovir and derivatives) (10, 48–51). The morbidity and socioeconomic burden associated with genital herpes, as well as the alarming relationship between genital herpes and HIV susceptibility, transmission and acquisition, all underscore the need for developing an effective HSV vaccine. The current medical opinion is that an effective clinical vaccine will constitute the best and cost-effective approach to protect the human population from genital herpes (50, 52, 53). Moreover, such a vaccine will likely have the greatest impact in both developed and developing regions of the world (49, 51, 52). To date, however, no prophylactic or therapeutic HSV vaccines for the prevention or treatment of genital herpes are available (53). Direct experiments in animal models (10, 54, 55) and indirect immunological observations from HSV infected human patients (56, 57) suggest that successful control of herpes infection is associated with induction of robust and polyfunctional CD8$^+$ T cells that reside within the vaginal sub-mucosal tissues (58). Our inability to efficiently design and deliver herpes antigens to stimulate strong local mucosal HSV-specific CD8$^+$ T cell responses remains a major obstacle in the development of an effective herpes vaccine. Given the limited success of antibody-mediated herpes vaccine in recent clinical trials, using protein-in-adjuvant vaccines delivered parenterally, it is an especially important finding that the CXCL17 mucosal chemokine promotes protective IFN-γ-producing cytotoxic CXCR8$^+$CD8$^+$ T$_{EM}$ and T$_{RM}$ cells in the VM (59). Consequently, the present findings are encouraging as they indicate CXCL17 chemokine as a possible mucosal adjuvant that can be included in a potential herpes prime/pull herpes vaccine to induce stronger mucosal immunity against genital herpes. Such prime/pull mucosal vaccine would be based on immunization with CD8$^+$ T cell epitopes to specifically induce functional HSV-specific CD8$^+$ T$_{EM}$ and T$_{RM}$ cell subsets combined with an intravaginal delivery of mucosal chemokines, such as CXCL17, that would mobilize these CD8$^+$ T$_{EM}$ and T$_{RM}$ cells into infected vaginal mucosa. The importance of CXCL17-CXCR8 is demonstrated in this study in B6 mouse strain, a genetic background on which CXCL17$^{-/-}$ deficient mice are currently available. It is important to demonstrate the importance of CXCL17-CXCR8 in other strains of mice once CXCL17$^{-/-}$ deficient mice are available on those genetic backgrounds.

In conclusion, our study represents the first in-depth analysis on the role of the CXCL17/CXCR8 pathway in anti-herpes T cell responses in the vaginal mucosa. Herein, we demonstrated that following intravaginal HSV-1 infection of B6 mice, a high production of CXCL17 chemokine in the vaginal mucosa was associated with the formation and the protective function of anti-viral IFN-γ-producing cytotoxic CXCR8$^+$CD8$^+$ T$_{EM}$ and T$_{RM}$ cells in the vaginal mucosa. In contrast, HSV-1 infection of CXCL17$^{-/-}$ deficient mice resulted in reduced numbers and frequencies of functional CXCR8$^+$CD8$^+$ T$_{EM}$ and T$_{RM}$ cells in the vaginal mucosa, which express markers of exhaustion, such as TIGIT and

VISTA. Less functional $CXCR8^+CD8^+$ T_{EM} and T_{RM} cells in the vaginal mucosa was associated with a failure to contain genital herpes infection and disease. Such observations could inform a combinatorial vaccine or immunotherapeutic approaches for genital herpes that would include intravaginal delivery of herpes antigens together with mucosal chemokines, such as CXCL17, and an immune checkpoint co-blockade. Such a combinatorial strategy would mobilize more functional $CD8^+$ T_{EM} and $CD8^+$ T_{RM} cells locally in the vaginal mucosa and, as such, would have a significant impact on genital herpes infection and disease.

Supplementary Material

Refer to Web version on PubMed Central for supplementary material.

Acknowledgments

References

1. Samandary S, Kridane-Miledi H, Sandoval JS, Choudhury Z, Langa-Vives F, SD, Chentoufi AA, Lemonnier FA, Benmohamed L. Associations of HLA-A, HLA-B and HLA-C Alleles Frequency with Prevalence of Herpes Simplex Virus Infections and Diseases Across Global Populations: Implication for the Development of an Universal CD8+ T-Cell Epitope-Based Vaccine. Human Immunology. 2014; 8:715–29.

2. Khan AA, Srivastava R, Lopes PP, Wang C, Pham TT, Cochrane J, Thai NT, Gutierrez L, Benmohamed L. Asymptomatic memory CD8 T cells: From development and regulation to consideration for human vaccines and immunotherapeutics. Hum Vaccin Immunotherapy. 2014; 10:945–63.

3. Dasgupta G, BenMohamed L. Of mice and not humans: how reliable are animal models for evaluation of herpes CD8(+)-T cell-epitopes-based immunotherapeutic vaccine candidates? Vaccine. 2011; 29:5824–5836. [PubMed: 21718746]

4. Bouley DM, Kanangat S, Wire W, Rouse BT. Characterization of herpes simplex virus type-1 infection and herpetic stromal keratitis development in IFN-gamma knockout mice. J Immunol. 1995; 155:3964–3971. [PubMed: 7561104]

5. Babu JS, Thomas J, Kanangat S, Morrison LA, Knipe DM, Rouse BT. Viral replication is required for induction of ocular immunopathology by herpes simplex virus. J Virol. 1996; 70:101–107. [PubMed: 8523513]

6. Deshpande SP, Lee S, Zheng M, Song B, Knipe D, Kapp JA, Rouse BT. Herpes simplex virus-induced keratitis: evaluation of the role of molecular mimicry in lesion pathogenesis. J Virol. 2001; 75:3077–3088. [PubMed: 11238834]

7. Khan AA, Srivastava R, Chentoufi AA, Kritzer E, Chilukuri S, Garg S, Yu DC, Vahed H, Huang L, Syed SA, Furness JN, Tran TT, Anthony NB, McLaren CE, Sidney J, Sette A, Noelle RJ, BenMohamed L. Bolstering the Number and Function of HSV-1-Specific CD8+ Effector Memory T Cells and Tissue-Resident Memory T Cells in Latently Infected Trigeminal Ganglia Reduces

Recurrent Ocular Herpes Infection and Disease. J Immunol. 2017; 199:186–203. [PubMed: 28539429]

8. van Velzen M, Jing L, Osterhaus AD, Sette A, Koelle DM, Verjans GM. Local CD4 and CD8 T-cell reactivity to HSV-1 antigens documents broad viral protein expression and immune competence in latently infected human trigeminal ganglia. PLoS Pathog. 2013; 9:e1003547. [PubMed: 23966859]

9. Samandary S, Kridane-Miledi H, Sandoval JS, Choudhury Z, Langa-Vives F, Spencer D, Chentoufi AA, Lemonnier FA, BenMohamed L. Associations of HLA-A, HLA-B and HLA-C alleles frequency with prevalence of herpes simplex virus infections and diseases across global populations: implication for the development of an universal CD8+ T-cell epitope-based vaccine. Hum Immunol. 2014; 75:715–729. [PubMed: 24798939]

10. Zhang X, Chentoufi AA, Dasgupta G, Nesburn AB, Wu M, Zhu X, Carpenter D, Wechsler SL, You S, BenMohamed L. A genital tract peptide epitope vaccine targeting TLR-2 efficiently induces local and systemic CD8+ T cells and protects against herpes simplex virus type 2 challenge. Mucosal Immunol. 2009; 2:129–143. [PubMed: 19129756]

11. Bettahi I, Zhang X, Afifi RE, BenMohamed L. Protective immunity to genital herpes simplex virus type 1 and type 2 provided by self-adjuvanting lipopeptides that drive dendritic cell maturation and elicit a polarized Th1 immune response. Viral Immunol. 2006; 19:220–236. [PubMed: 16817765]

12. Shin H, Iwasaki A. A vaccine strategy that protects against genital herpes by establishing local memory T cells. Nature. 2012; 491:463–467. [PubMed: 23075848]

13. Zhang X, Dervillez X, Chentoufi AA, Badakhshan T, Bettahi I, Benmohamed L. Targeting the genital tract mucosa with a lipopeptide/recombinant adenovirus prime/boost vaccine induces potent and long-lasting CD8+ T cell immunity against herpes: importance of MyD88. J Immunol. 2012; 189:4496–4509. [PubMed: 23018456]

14. Schenkel JM, Fraser KA, Masopust D. Cutting edge: resident memory CD8 T cells occupy frontline niches in secondary lymphoid organs. J Immunol. 2014; 192:2961–2964. [PubMed: 24600038]

15. Schenkel JM, Fraser KA, Beura LK, Pauken KE, Vezys V, Masopust D. T cell memory. Resident memory CD8 T cells trigger protective innate and adaptive immune responses. Science. 2014; 346:98–101. [PubMed: 25170049]

16. Hernandez-Ruiz M, Zlotnik A, Llorente L, Hernandez-Molina G. Markedly high salivary and lacrimal CXCL17 levels in primary Sjogren's syndrome. Joint Bone Spine. 2017; 17:30105–7.

17. Hernandez-Ruiz M, Zlotnik A. Mucosal Chemokines. J Interferon Cytokine Res. 2017; 37:62–70. [PubMed: 28207301]

18. Lee WY, Wang CJ, Lin TY, Hsiao CL, Luo CW. CXCL17, an orphan chemokine, acts as a novel angiogenic and anti-inflammatory factor. American journal of physiology Endocrinology and metabolism. 2013; 304:E32–40. [PubMed: 23115081]

19. Maravillas-Montero JL, Burkhardt AM, Hevezi PA, Carnevale CD, Smit MJ, Zlotnik A. Cutting edge: GPR35/CXCR8 is the receptor of the mucosal chemokine CXCL17. J Immunol. 2015; 194:29–33. [PubMed: 25411203]

20. Pisabarro MT, Leung B, Kwong M, Corpuz R, Frantz GD, Chiang N, Vandlen R, Diehl LJ, Skelton N, Kim HS, Eaton D, Schmidt KN. Cutting edge: novel human dendritic cell- and monocyte-attracting chemokine-like protein identified by fold recognition methods. Journal of immunology. 2006; 176:2069–2073.

21. Burkhardt AM, Tai KP, Flores-Guiterrez JP, Vilches-Cisneros N, Kamdar K, Barbosa-Quintana O, Valle-Rios R, Hevezi PA, Zuniga J, Selman M, Ouellette AJ, Zlotnik A. CXCL17 is a mucosal chemokine elevated in idiopathic pulmonary fibrosis that exhibits broad antimicrobial activity. Journal of immunology. 2012; 188:6399–6406.

22. Deng J, Yao Z, Chen K, Yuan YA, Lin J, Wei D. Towards the computational design and engineering of enzyme enantioselectivity: A case study by a carbonyl reductase from Gluconobacter oxydans. J Biotechnol. 2016; 217:31–40. [PubMed: 26590330]

23. Gebhardt T, Whitney PG, Zaid A, Mackay LK, Brooks AG, Heath WR, Carbone FR, Mueller SN. Different patterns of peripheral migration by memory CD4+ and CD8+ T cells. Nature. 2011; 477:216–219. [PubMed: 21841802]

24. Mueller SN, Gebhardt T, Carbone FR, Heath WR. Memory T cell subsets, migration patterns, and tissue residence. Annu Rev Immunol. 2013; 31:137–161. [PubMed: 23215646]

25. Steinert EM, Schenkel JM, Fraser KA, Beura LK, Manlove LS, Igyarto BZ, Southern PJ, Masopust D. Quantifying Memory CD8 T Cells Reveals Regionalization of Immunosurveillance. Cell. 2015; 161:737–749. [PubMed: 25957682]

26. Parr MB, Parr EL. Protective immunity against HSV-2 in the mouse vagina. J Reprod Immunol. 1997; 36:77–92. [PubMed: 9430740]

27. Iijima N, Linehan MM, Zamora M, Butkus D, Dunn R, Kehry MR, Laufer TM, Iwasaki A. Dendritic cells and B cells maximize mucosal Th1 memory response to herpes simplex virus. J Exp Med. 2008; 205:3041–3052. [PubMed: 19047439]

28. Chauvin JM, Pagliano O, Fourcade J, Sun Z, Wang H, Sander C, Kirkwood JM, Chen TH, Maurer M, Korman AJ, Zarour HM. TIGIT and PD-1 impair tumor antigen-specific CD8(+) T cells in melanoma patients. J Clin Invest. 2015; 125:2046–2058. [PubMed: 25866972]

29. Lines JL, Pantazi E, Mak J, Sempere LF, Wang L, O'Connell S, Ceeraz S, Suriawinata AA, Yan S, Ernstoff MS, Noelle R. VISTA is an immune checkpoint molecule for human T cells. Cancer Res. 2014; 74:1924–1932. [PubMed: 24691993]

30. Wang L, Rubinstein R, Lines JL, Wasiuk A, Ahonen C, Guo Y, Lu LF, Gondek D, Wang Y, Fava RA, Fiser A, Almo S, Noelle RJ. VISTA, a novel mouse Ig superfamily ligand that negatively regulates T cell responses. J Exp Med. 2011; 208:577–592. [PubMed: 21383057]

31. Zhu J, Peng T, Johnston C, Phasouk K, Kask AS, Klock A, Jin L, Diem K, Koelle DM, Wald A, Robins H, Corey L. Immune surveillance by CD8alphaalpha+ skin-resident T cells in human herpes virus infection. Nature. 2013; 497:494–497. [PubMed: 23657257]

32. Zhu J, Peng T, Johnston C, Phasouk K, Kask AS, Klock A, Jin L, Diem K, Koelle DM, Wald A, Robins H, Corey L. Immune surveillance by CD8alphaalpha skin-resident T cells in human herpes virus infection. Nature. 2013; 497:494–7. [PubMed: 23657257]

33. Schiffer JT, Abu-Raddad L, Mark KE, Zhu J, Selke S, Koelle DM, Wald A, Corey L. Mucosal host immune response predicts the severity and duration of herpes simplex virus-2 genital tract shedding episodes. Proc Natl Acad Sci U S A. 2010; 107:18973–18978. [PubMed: 20956313]

34. Zhu J, Hladik F, Woodward A, Klock A, Peng T, Johnston C, Remington M, Magaret A, Koelle DM, Wald A, Corey L. Persistence of HIV-1 receptor-positive cells after HSV-2 reactivation is a potential mechanism for increased HIV-1 acquisition. Nat Med. 2009; 15:886–892. [PubMed: 19648930]

35. Zhu J, Koelle DM, Cao J, Vazquez J, Huang ML, Hladik F, Wald A, Corey L. Virus-specific CD8+ T cells accumulate near sensory nerve endings in genital skin during subclinical HSV-2 reactivation. J Exp Med. 2007; 204:595–603. [PubMed: 17325200]

36. Tang VA, Rosenthal KL. Intravaginal infection with herpes simplex virus type-2 (HSV-2) generates a functional effector memory T cell population that persists in the murine genital tract. J Reprod Immunol. 2010; 87:39–44. [PubMed: 20688399]

37. Peng T, Zhu J, Phasouk K, Koelle DM, Wald A, Corey L. An effector phenotype of CD8+ T cells at the junction epithelium during clinical quiescence of herpes simplex virus 2 infection. J Virol. 2012; 86:10587–10596. [PubMed: 22811543]

38. Ariotti S, Hogenbirk MA, Dijkgraaf FE, Visser LL, Hoekstra ME, Song JY, Jacobs H, Haanen JB, Schumacher TN. T cell memory. Skin-resident memory CD8(+) T cells trigger a state of tissue-wide pathogen alert. Science. 2014; 346:101–105. [PubMed: 25278612]

39. Mackay LK, Rahimpour A, Ma JZ, Collins N, Stock AT, Hafon ML, Vega-Ramos J, Lauzurica P, Mueller SN, Stefanovic T, Tscharke DC, Heath WR, Inouye M, Carbone FR, Gebhardt T. The developmental pathway for CD103CD8 tissue-resident memory T cells of skin. Nat Immunol. 2013; 14:1294–301. [PubMed: 24162776]

40. Mackay LK, Rahimpour A, Ma JZ, Collins N, Stock AT, Hafon ML, Vega-Ramos J, Lauzurica P, Mueller SN, Stefanovic T, Tscharke DC, Heath WR, Inouye M, Carbone FR, Gebhardt T. The developmental pathway for CD103(+)CD8+ tissue-resident memory T cells of skin. Nature immunology. 2013; 14:1294–1301. [PubMed: 24162776]

41. Wakim LM, Woodward-Davis A, Liu R, Hu Y, Villadangos J, Smyth G, Bevan MJ. The molecular signature of tissue resident memory CD8 T cells isolated from the brain. J Immunol. 2012; 189:3462–3471. [PubMed: 22922816]

42. Gebhardt T, Mackay LK. Local immunity by tissue-resident CD8(+) memory T cells. Front Immunol. 2012; 3:340. [PubMed: 23162555]

43. Mackay LK, Wakim L, van Vliet CJ, Jones CM, Mueller SN, Bannard O, Fearon DT, Heath WR, Carbone FR. Maintenance of T cell function in the face of chronic antigen stimulation and repeated reactivation for a latent virus infection. J Immunol. 2012; 188:2173–2178. [PubMed: 22271651]

44. Mackay LK, Wakim L, van Vliet CJ, Jones CM, Mueller SN, Bannard O, Fearon DT, Heath WR, Carbone FR. Maintenance of T Cell Function in the Face of Chronic Antigen Stimulation and Repeated Reactivation for a Latent Virus Infection. J Immunol. 2012

45. Mackay LK, Stock AT, Ma JZ, Jones CM, Kent SJ, Mueller SN, Heath WR, Carbone FR, Gebhardt T. Long-lived epithelial immunity by tissue-resident memory T (TRM) cells in the absence of persisting local antigen presentation. Proc Natl Acad Sci U S A. 2012; 109:7037–7042. [PubMed: 22509047]

46. Weinstein EJ, Head R, Griggs DW, Sun D, Evans RJ, Swearingen ML, Westlin MM, Mazzarella R. VCC-1, a novel chemokine, promotes tumor growth. Biochem Biophys Res Commun. 2006; 350:74–81. [PubMed: 16989774]

47. Chew GM, Fujita T, Webb GM, Burwitz BJ, Wu HL, Reed JS, Hammond KB, Clayton KL, Ishii N, Abdel-Mohsen M, Liegler T, Mitchell BI, Hecht FM, Ostrowski M, Shikuma CM, Hansen SG, Maurer M, Korman AJ, Deeks SG, Sacha JB, Ndhlovu LC. TIGIT Marks Exhausted T Cells, Correlates with Disease Progression, and Serves as a Target for Immune Restoration in HIV and SIV Infection. PLoS Pathog. 2016; 12:e1005349. [PubMed: 26741490]

48. Dasgupta G, Nesburn AB, Wechsler SL, BenMohamed L. Developing an asymptomatic mucosal herpes vaccine: the present and the future. Future Microbiol. 2010; 5:1–4. [PubMed: 20020824]

49. Zhang X, Castelli FA, Zhu X, Wu M, Maillere B, BenMohamed L. Gender-dependent HLA-DR-restricted epitopes identified from herpes simplex virus type 1 glycoprotein D. Clinical and vaccine immunology : CVI. 2008; 15:1436–1449. [PubMed: 18667634]

50. Dasgupta G, Chentoufi AA, Kalantari-Dehaghi M, Falatoonzadeh P, Chun S, LCH, Felgner PL, HDH, BenMohamed L. Immunodominant "Asymptomatic" Herpes Simplex Virus Type 1 and Type 2 Protein Antigens Identified by Probing Whole ORFome Microarrays By Serum Antibodies From Seropositive Asymptomatic Versus Symptomatic Individuals. J Virology. 2012; 86:4358–69. [PubMed: 22318137]

51. Chentoufi AA, Kritzer E, YMD, Nesburn AB, BenMohamed L. Towards a Rational Design of an Asymptomatic Clinical Herpes Vaccine: The Old, The New, and The Unknown. Clinical and Developmental Immunology. 2012; 12:187–199.

52. Kalantari-Dehaghi M, Chun S, Chentoufi AA, Pablo J, LL, Dasgupta G, DM, Jasinskas A, Nakajimi-sasaki R, Felgner J, Hermanson G, BenMohamed L, Felgner PL, HDH. Discovery of potential diagnostic and vaccine antigens in herpes simplex virus-1 and -2 by proteome-wide antibody profiling. J Virology. 2012; 86:4328–39. [PubMed: 22318154]

53. Dervillez X, Wechsler S, Nesburn AB, BenMohamed L. Future of an "Asymptomatic" T-cell Epitope-Based Therapeutic Herpes Simplex Vaccine. Future Virology. 2012; 7:371–378. [PubMed: 22701511]

54. Cohen J. Immunology. Painful failure of promising genital herpes vaccine. Science. 2010; 330:304. [PubMed: 20947733]

55. King NJ, Parr EL, Parr MB. Migration of lymphoid cells from vaginal epithelium to iliac lymph nodes in relation to vaginal infection by herpes simplex virus type 2. J Immunol. 1998; 160:1173–1180. [PubMed: 9570531]

56. Zhao X, Deak E, Soderberg K, Linehan M, Spezzano D, Zhu J, Knipe DM, Iwasaki A. Vaginal submucosal dendritic cells, but not Langerhans cells, induce protective Th1 responses to herpes simplex virus-2. J Exp Med. 2003; 197:153–162. [PubMed: 12538655]

57. Koelle DM, Posavad CM, Barnum GR, Johnson ML, Frank JM, Corey L. Clearance of HSV-2 from recurrent genital lesions correlates with infiltration of HSV-specific cytotoxic T lymphocytes. J Clin Invest. 1998; 101:1500–1508. [PubMed: 9525993]

58. Posavad CM, Koelle DM, Shaughnessy MF, Corey L. Severe genital herpes infections in HIV-infected individuals with impaired herpes simplex virus-specific CD8+ cytotoxic T lymphocyte responses. Proc Natl Acad Sci U S A. 1997; 94:10289–10294. [PubMed: 9294203]

59. Jing L, Haas J, Chong TM, Bruckner JJ, Dann GC, Dong L, Marshak JO, McClurkan CL, Yamamoto TN, Bailer SM, Laing KJ, Wald A, Verjans GM, Koelle DM. Cross-presentation and genome-wide screening reveal candidate T cells antigens for a herpes simplex virus type 1 vaccine. J Clin Invest. 2012; 122:654–673. [PubMed: 22214845]

60. Mestecky J, Fultz PN. Mucosal immune system of the human genital tract. The Journal of infectious diseases. 1999; 179(Suppl 3):S470–474. [PubMed: 10099122]
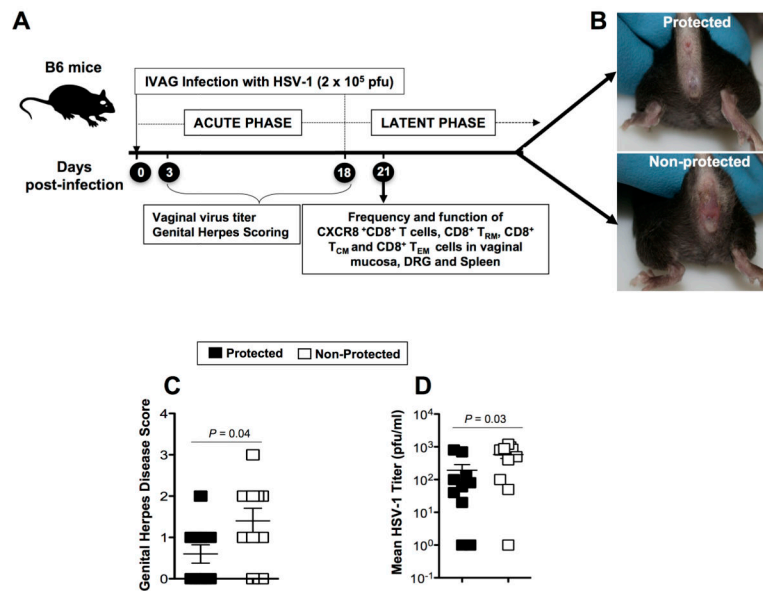
Figure 1. Intravaginal infection of B6 mice with a 2×10^5 dose of HSV-1 (strain McKrae) leads to protected animals, with no herpetic disease, and non-protected animals with severe genital herpetic disease

(**A**) Schedule of HSV-1 intravaginal infection and subsequent immunological and virological analyses. B6 mice (5–6 wk. old, $n = 30$) were treated with Depo-Provera® and then infected intra-vaginally on day 0 with 2×10^5 pfu of HSV-1 (strain McKrae). Vaginal washes were collected from day 3 to day 18 post infection. The presence of infectious virus in the vaginal washes was determined by plaque assay. (**B**) Representative pictures of an infected/protected mouse with no genital lesions (*top*) and of infected/non-protected mouse with genital acute herpetic lesions (*bottom*). (**C**) Starting on day 3 post-infection with HSV-1, the severity of acute genital herpetic disease is scored daily on a scale of 0 to 4. (**D**) Vaginal washes were collected from day 3 to day 18, during the acute phase of infection, from both protected and non-protected mice. Shown are optimal infectious virus particles quantified, on day 6 post-infection, by plaque assay in the vaginal wash samples of protected and non-protected mice. The data are representative of two independent experiments and the bars represent SD between the experiments. Differences between the groups were identified by ANOVA, multiple comparison procedures, as we previously described (10). The indicated *P* values show statistical significance between protected and non-protected mice.
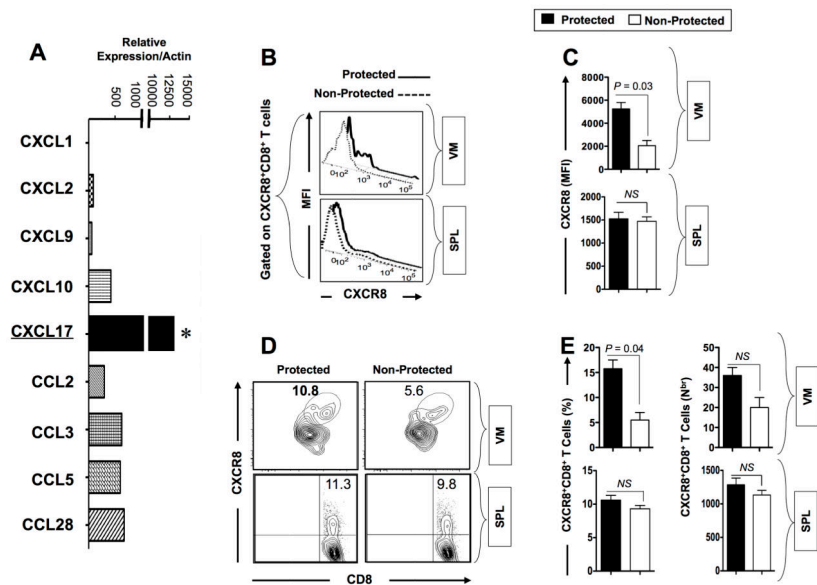
Figure 2. High levels of CXCL17 chemokine and frequent CD8^{+} T cells, expressing CXCR8, the cognate receptor of CXCL17, are detected in the vaginal mucosa of HSV-1 infected and protected mice

(**A**) Levels of mucosal and T-cell attracting chemokines detected in the vaginal mucosa of HSV infected mice. Mice ($n = 10$) were intravaginally infected with HSV-1, euthanized on day 21 post infection and single cell suspension from vaginal mucosa were obtained after collagenase treatment. Vaginal cell suspensions ($\sim 10 \times 10^6$) were analyzed by PCR for the indicated chemokines. (**B** to **E**) Mice were euthanized on day 21 post infection and single cell suspension from vaginal mucosa and spleen (control) were stained for CXCR8 and CD8^{+} T cells markers and analyzed by FACS. Representative (**B**) and (**C**) average levels of expression of CXCR8 receptor on CD8^{+} T cells from the vaginal mucosa (*top panels*) and spleen (*bottom panels*) of protected versus non-protected mice. (**D**) Representative FACS plot of the frequency of CXCR8^{+}CD8^{+} T cells detected in the vaginal mucosa (*top panels*) and spleen (*bottom panels*) of protected versus non-protected mice. (**E**) Average frequencies (*left*) and absolute numbers (*right*) of CXCR8^{+}CD8^{+} T cells in the vaginal mucosa and spleen of protected versus non-protected mice. Differences between the groups were identified by ANOVA, multiple comparison procedures. The data are representative of two independent experiments. The indicated *P* values show statistical significance between protected and non-protected mice.
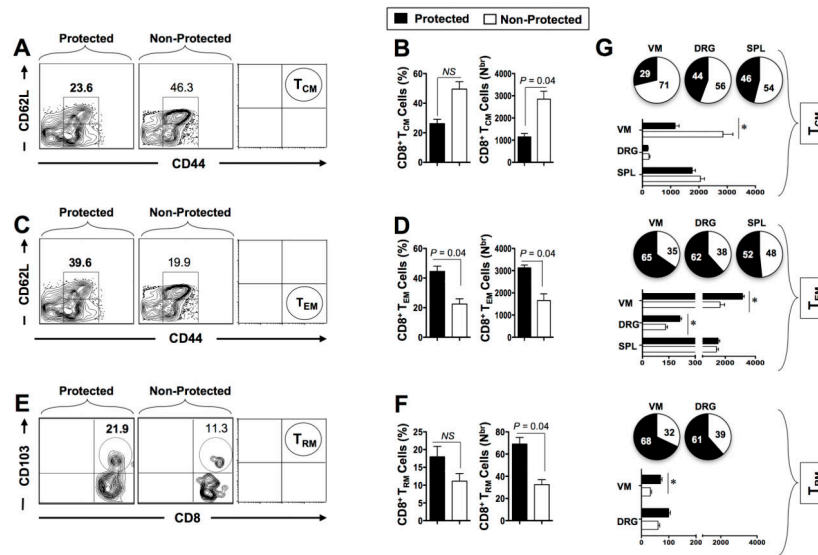
Figure 3. Frequent CD44^{high}CCR7^{low}CD8$^+$ T$_{EM}$ and CD103^{high}CCR7^{low}CD62L^{low}CD8$^+$ T$_{RM}$ cells detected in the vaginal mucosa of HSV-1 infected/protected B6 mice

(**A**) Representative FACS data of the frequencies of HSV-1 gB$_{498–505}$-specific CD44^{high}CD62L^{high}CD8$^+$ T$_{CM}$ cells detected in the vaginal mucosa (VM) from one HSV-1 infected protected and one non-protected mouse. (**B**) Average frequencies (*left*) and absolute numbers (*right*) of T$_{CM}$ cells detected in the VM from 10 HSV-1 infected protected and non-protected mice. (**C**) Representative FACS data of the frequencies of HSV-1 gB$_{498–505}$-specific CD44^{high}CD62L^{low}CD8$^+$ T$_{EM}$ cells detected in the VM from one HSV-1 infected protected and one non-protected mouse. (**D**) Average frequencies (*left*) and numbers (*right*) of T$_{EM}$ cells detected in the VM from 10 protected and 10 non-protected mice. (**E**) Representative FACS data of the frequencies of HSV-1 gB$_{498–505}$-specific CD103^{high}CCR7^{low}CD62L^{low}CD8$^+$ T$_{RM}$ cells detected in the VM from one HSV-1 infected protected and one non-protected mouse. (**F**) Average frequencies (*left*) and numbers (*right*) of CD8$^+$ T$_{RM}$ cells detected in the VM from 10 protected and 10 non-protected mice. (**G**) Each pie chart and bar graphs represents the overall mean of absolute numbers of different subsets of HSV-1 gB$_{498–505}$-specific memory CD8$^+$T cells (T$_{CM}$, T$_{EM}$ and T$_{RM}$) detected in vaginal mucosa (VM), dorsal root ganglia (DRG) and spleen (SPL) of protected versus non-protected mice. The results are representative of two independent experiments. Differences between the groups were identified by ANOVA, multiple comparison procedures. The indicated *P* values show statistical significance between protected and non-protected mice.
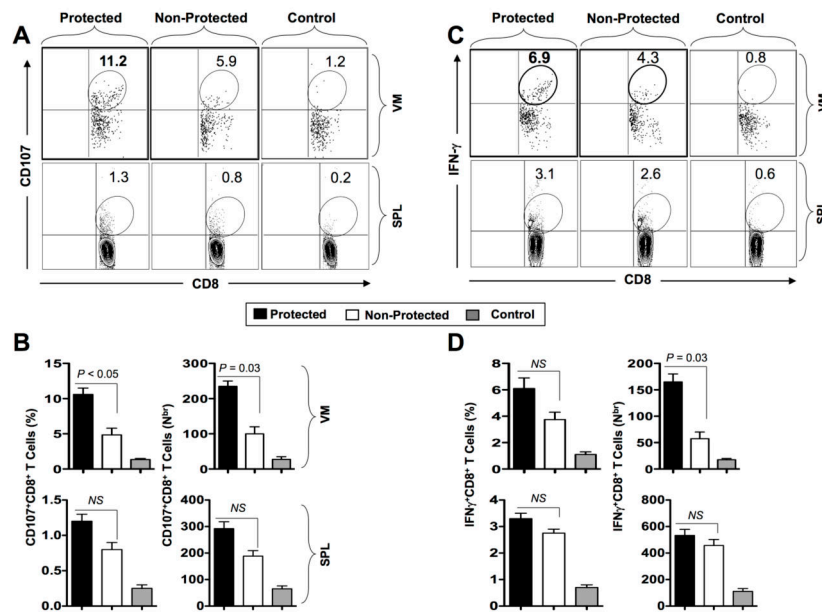
Figure 4. Functional CD8+ T cells in the vaginal mucosa of HSV-1 infected/protected B6 mice

Single cell suspension from the VM, obtained after collagenase treatment, and SPL were harvested from protected and non-protected B6 mice on day 21 post-infection. The VM and SPL cell were stained for CD8+ T cells, tetramer specific for the HSV-1 gB$_{498-505}$ epitope and for CD107 marker of cytotoxicity and IFN-γ production and then analyzed by FACS. (**A**) Representative FACS data of the frequencies of CD107+CD8+ T cells detected in the VM (*top panels*) and SPL (*bottom panels*) of protected versus non-protected mice and control cells from VM and SPL that were not stimulated with peptide (*right panels*) (**B**) Average frequencies (*left panels*) and absolute numbers (*middle panels*) of CD107+CD8+ T cells in the VM and SPL of 10 protected and 10 non-protected mice. (**C**) Representative FACS data of the frequencies of IFN-γ+CD8+ T cells detected in the VM (*top panels*) and SPL (*bottom panels*) of protected versus non-protected mice. (**D**) Average frequencies (*left panels*) and absolute number (*middle panels*) of IFN-γ+CD8+ T cells in the VM and SPL of 10 protected and 10 non-protected mice. Control cells from VM and SPL that were not stimulated with peptide are shown in (*right panels*). Results are representative of two independent experiments. Differences between the groups were identified by ANOVA, multiple comparison procedures. The indicated *P* values show statistical significance between protected and non-protected mice.
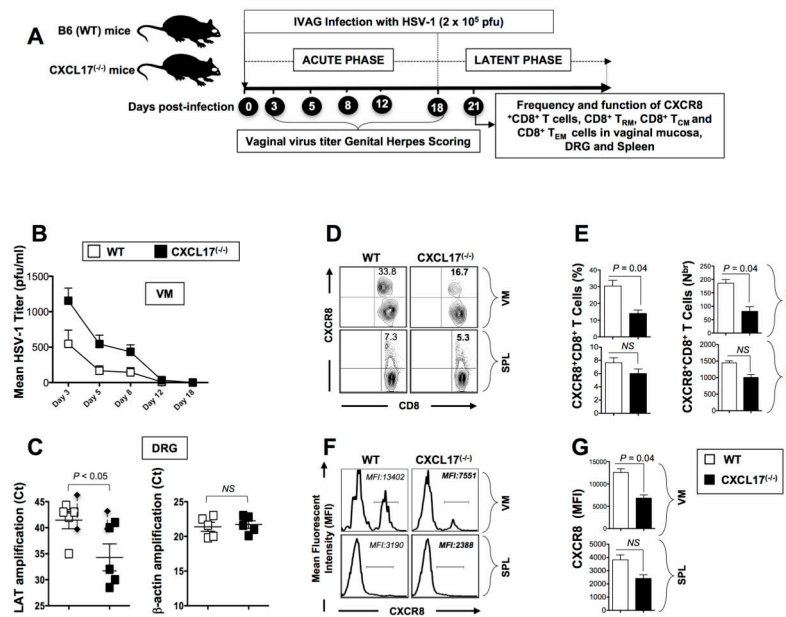
Figure 5. Lack of CXCL17 compromises the mobilization of memory CXCR8⁺CD8⁺ T cells in the vaginal mucosa of HSV-1 infected CXCL17$^{(-/-)}$ mice

(**A**) Schedule of HSV-1 intravaginal infection and subsequent immunological and virological analyses. CXCL17$^{(-/-)}$ deficient mice and B6 wild type (WT) mice (5–6 wk. old, $n = 10$) were treated with Depo-Provera® and then infected intra-vaginally on day 0 with 2×10^5 pfu of HSV-1 (strain McKrae). (**B**) Average virus titers detected in the vaginal washes collected from day 3 to day 18 post infection from CXCL17$^{(-/-)}$ and WT mice. The presence of infectious viral particles in the vaginal mucosa (VM) was determined by plaque assay. (**C**) The level of latency in the dorsal root ganglia (DRG) was determined by assessing expression level of latency associated transcript (LAT) gene (*left panel*). β-actin gene was used as control (*right panel, control*). Results are plotted as real-time PCR C_T (cycle of threshold) values. The dotted arrow lines indicate lack transcript amplification around 40 PCR cycles. (**D**–**G**) Show frequency of CXCR8⁺CD8⁺ T cells and level of expression of CXCL17 receptor on CD8⁺ T cells were analyzed by FACS in the vaginal mucosa. HSV infected CXCL17$^{(-/-)}$ versus WT mice were euthanized on day 21 post-infection and single cell suspension obtained from the VM and SPL (control). (**D**) Representative FACS plot of the frequency of CXCR8⁺CD8⁺ T cells detected in the VM (*top panels*) and SPL (*bottom panels*) of one WT mouse versus one CXCL17$^{(-/-)}$ mouse. (**E**) Average percentages (*left panels*) and absolute numbers (*right panels*) of CXCR8⁺CD8⁺ T cells in the VM (*top panels*) and SPL (*bottom panels*) of ten WT mice and ten CXCL17$^{(-/-)}$. (**F** and **G**) Levels of expression of CXCR8 receptor on CD8⁺ T cells from VM (*top panels*) and SPL (*bottom panels*) of WT versus CXCL17$^{(-/-)}$ mice. The data are representative of two independent experiments. Differences between the groups were identified by ANOVA, multiple comparison procedures. The indicated *P* values show statistical significance between CXCL17$^{(-/-)}$ versus WT mice.
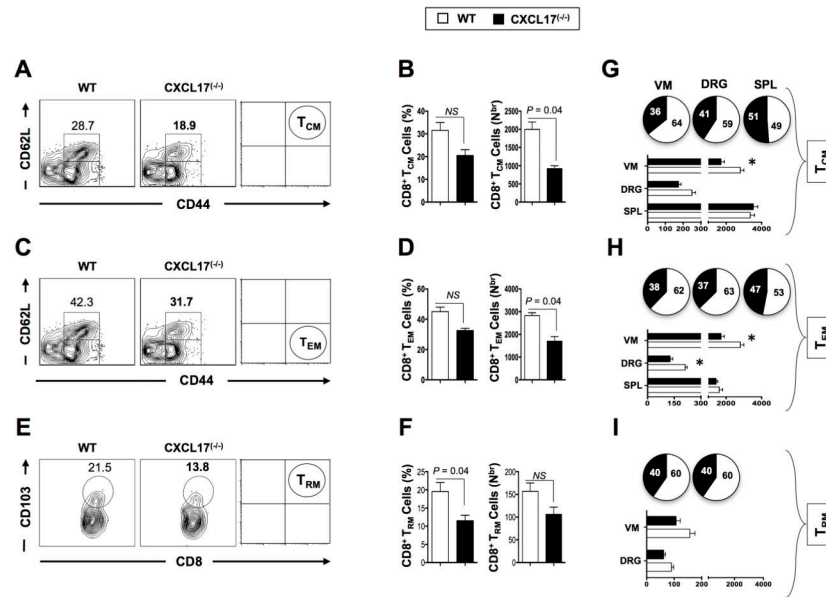
Figure 6. Less CD8$^+$ T$_{CM}$, T$_{EM}$ and T$_{RM}$ cells are mobilized in the vaginal mucosa of HSV-1 infected CXCL17$^{(-/-)}$ deficient mice compared to WT mice

A group of 10 age-matched CXCL17$^{(-/-)}$ and WT female mice were treated with Depo-Provera® and subsequently infected intra-vaginally on day 0 with 2×10^5 pfu of HSV-1 (as in Fig. 5A). Mice were euthanized on day 21 post infection and single cell suspension from vaginal mucosa (VM), dorsal roots ganglia (DRG) and spleen (SPL) were stained for the 3 major subsets of memory CD8$^+$ cells (i.e. T$_{CM}$, T$_{EM}$ and T$_{RM}$ cells) and analyzed by FACS. (**A**) Representative FACS data of the frequencies of HSV-1 gB$_{498-505}$-specific CD44^{high}CD62L^{high}CD8$^+$ T$_{CM}$ cells detected in the VM from one HSV-1 infected WT mouse and one CXCL17$^{(-/-)}$ mouse. (**B**) Average frequencies (*left panel*) and numbers (*right panel*) of CD8$^+$ T$_{CM}$ cells detected in the VM from 10 HSV-1 infected WT mice and 10 CXCL17$^{(-/-)}$ mice. (**C**) Representative FACS data of the frequencies of gB$_{498-505}$-specific CD44^{high}CD62L^{low}CD8$^+$ T$_{EM}$ cells detected in the VM from one HSV-1 infected WT and one CXCL17$^{(-/-)}$ mouse. (**D**) Average frequencies (*left panel*) and numbers (*right panel*) of CD8$^+$ T$_{EM}$ cells detected in the VM from 10 HSV-1 infected WT and CXCL17$^{(-/-)}$ mice. (**E**) Representative FACS data of the frequencies of HSV-1 gB$_{498-505}$-specific CD103^{high}CCR7^{low}CD62L^{low}CD8$^+$ T$_{RM}$ cells detected in the VM from one HSV-1 infected WT and one CXCL17$^{(-/-)}$ mouse. (**F**) Average frequencies (*left panel*) and numbers (*right panel*) of CD8$^+$ T$_{RM}$ cells detected in the VM from 10 HSV-1 infected WT and CXCL17$^{(-/-)}$ mice. The percentages (*pie charts*) and the mean of absolute numbers (*bar graphs*) of memory CD8$^+$ T$_{CM}$ cells (**G**), of memory CD8$^+$ T$_{EM}$ cells (**H**), and of memory CD8$^+$ T$_{RM}$ cells (**I**) detected in the VM, DRG and SPL compartment of WT mice (*white*) vs. CXCL17$^{(-/-)}$ mice (*black*). The results are representative of 2 independent experiments. Differences between the groups were identified by ANOVA, multiple comparison procedures. The indicated *P* values show statistical significance between CXCL17$^{(-/-)}$ and WT mice.
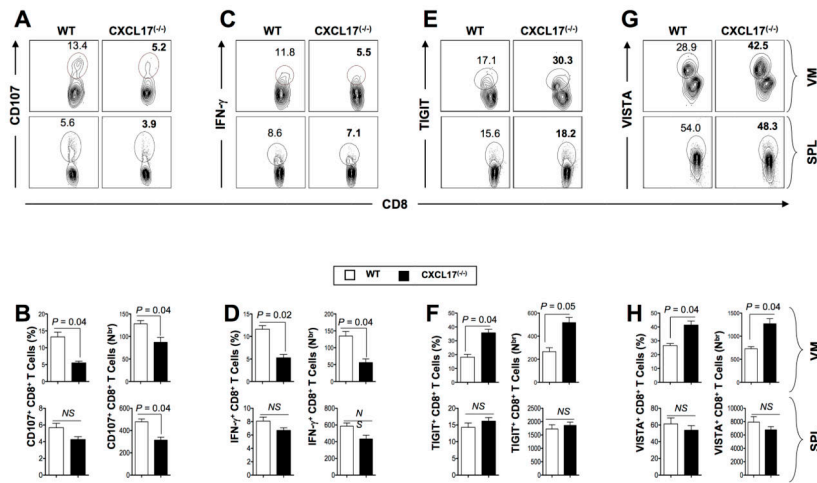
Figure 7. CXCL17 deficiency resulted in reduction in the number and frequency of functional CD8$^+$ T cells in the vaginal mucosa

Single cell suspension from VM and SPL were obtained on day 21 post-infection and stained for CD107, marker of cytotoxicity, IFN-γ, and two markers of exhaustion TIGIT and VISTA, and then analyzed by FACS. (**A**) Representative dot plots of the frequencies of CD107$^+$CD8$^+$ T cells detected in the VM (*top panels*) and SPL (*bottom panels*) of HSV-1 infected CXCL17$^{(-/-)}$ vs. WT mice. (**B**) Average frequencies (*left panels*) and absolute number (*right panels*) of CD107$^+$CD8$^+$ T cells in VM (*top panel*) and in SPL (*bottom panel*) of 10 CXCL17$^{(-/-)}$ vs. 10 WT mice. (**C**) Representative dot plots of the frequencies of IFN-γ$^+$CD8$^+$ T cells detected in the VM (*top panels*) and SPL (*bottom panels*) of HSV-1 infected CXCL17$^{(-/-)}$ vs. WT mice. (**D**) Average frequencies (*left panels*) and absolute number (*right panels*) of IFN-γ$^+$CD8$^+$ T cells in VM (*top panel*) and in SPL (*bottom panel*) of 10 CXCL17$^{(-/-)}$ vs. 10 WT mice. (**E**) Representative dot plots of the frequencies of TIGIT$^+$CD8$^+$ T cells detected in the VM (*top panels*) and in the SPL (*bottom panels*) of HSV-1 infected CXCL17$^{(-/-)}$ vs. WT mice. (**F**) Average frequencies (*left panels*) and absolute number (*right panels*) of TIGIT$^+$CD8$^+$ T cells in VM (*top panel*) and in SPL (*bottom panel*) of 10 CXCL17$^{(-/-)}$ vs. 10 WT mice. (**G**) Representative dot plots of the frequencies of VISTA$^+$CD8$^+$ T cells detected in the VM (*top panels*) and in the SPL (*bottom panels*) of HSV-1 infected CXCL17$^{(-/-)}$ vs. WT mice. (**F**) Average frequencies (*left panels*) and absolute number (*right panels*) of VISTA$^+$CD8$^+$ T cells in VM (*top panel*) and in SPL (*bottom panel*) of 10 CXCL17$^{(-/-)}$ vs. 10 WT mice. The results are representative of 2 independent experiments. Differences between the groups were identified by ANOVA, multiple comparison procedures. The indicated *P* values show statistical significance between CXCL17$^{(-/-)}$ vs. WT mice.